Rev.Adv.Mater.Sci. 25 (2010) 249-255

# CHARACTERISTICS OF CAVITATION IN A SUPERPLASTIC MAGNESIUM AZ31 ALLOY PROCESSED BY EQUAL-CHANNEL ANGULAR PRESSING

**Roberto B. Figueiredo[1] and Terence G. Langdon[1,2]**

[1]Materials Research Group, School of Engineering Sciences, University of Southampton, Southampton SO17 1BJ, UK
[2]Departments of Aerospace & Mechanical Engineering and Materials Science, University of Southern California, Los Angeles, CA 90089-1453, USA

*Received: November 05, 2009*

**Abstract.** Experiments were conducted on a magnesium AZ31 alloy to evaluate the role of cavitation in high temperature superplasticity. Samples were processed by equal-channel angular pressing (ECAP) and then pulled to failure in tension at a temperature of 623K. Similar tests were also conducted on the as-received alloy. The results show the development of significant internal cavitation in this alloy when testing both the as-received samples and the samples processed by ECAP at strain rates up to $10^{-3}$ $s^{-1}$. An analysis of the cavity morphologies shows the cavities grow initially by a diffusion process in which vacancies are absorbed from the surrounding grain boundaries but there is a transition to plasticity-controlled growth for the larger cavities.

## 1. INTRODUCTION

Equal-Channel Angular Pressing (ECAP) is recognized as an effective processing tool for refining the grain structure of metallic materials [1]. A direct consequence of the fine or ultrafine grain structures produced by this technique is the introduction of superplastic capabilities in many alloys when testing in tension at elevated temperatures. For example, a recent review documented more than sixty reports of superplastic flow in metals processed by ECAP [2]. Despite the early success in introducing superplasticity in many f.c.c. alloys, the occurrence of superplastic flow in magnesium alloys is a very recent development. This is primarily due to the difficulty of effectively processing magnesium alloys to attain grain refinement [3], the need to develop alternative processing routes such as the two-step EX-ECAP (extrusion and equal-channel angular pressing) procedure [4,5] and the realization that pressing may be conducted more effectively by increasing the strain rate sensitivity and/or by increasing the channel angle within the ECAP die [6].

The processing routes for the production of fine or ultrafine grain structures in magnesium alloys are now established and this has led to an interest in attaining superplastic properties in these materials. A recent report described exceptional superplasticity in a commercial ZK60 alloy processed by ECAP with an elongation of 3050% when testing at a tem-

Corresponding author: Roberto B. Figueiredo, e-mail: R.Figueiredo@soton.ac.uk

perature of 473K [7]: this elongation is not only the highest reported to date for any magnesium alloy processed under any conditions but it is also the highest elongation reported for any metallic alloy processed by ECAP. It has been shown that this record elongation is due to the pronounced strain hardening and strain rate sensitivity that inhibits the development of sharp necking during superplastic flow for the ZK60 alloy [7,8].

The ZK60 alloy exhibits superplasticity at relatively low temperatures in the range of ~450-550K after processing by ECAP and at these temperatures the alloy exhibits significant resistance to the development of internal cavitation. However, the magnesium AZ31 alloy appears to exhibit superplasticity at significantly higher temperatures, typically above ~600K [9], with a recent report documenting a superplastic elongation of 1210% when testing at a temperature of 623K [10]. Some preliminary experimental results are available describing the formation of cavities in the tensile testing of AZ31 alloys both after extrusion without ECAP [11] and after processing by ECAP [12]. However, to date there has been no detailed analysis of the cavity growth mechanisms occurring in any magnesium-based alloys although this type of analysis was reported earlier for an aluminum alloy [13] and an aluminum metal matrix composite [14] after processing by ECAP. Accordingly, the present research was undertaken to obtain quantitative information on the formation and growth of cavities during the high temperature deformation of a superplastic magnesium AZ31 alloy processed by ECAP.

## 2. EXPERIMENTAL MATERIAL AND PROCEDURES

The material used in this work was the commercial AZ31 (Mg-3 wt.% Al-1 wt.% Zn) alloy. The material was received as extruded rods having a diameter of 10 mm and these rods were cut into billets having lengths of 60 mm. In the as-received condition, the mean linear intercept grain size, $\bar{L}$, was ~9.1 μm where this is equivalent to an average spatial grain size, $d$ (= 1.74 · $\bar{L}$), of ~15.8 μm.

Several earlier reports described the processing of the AZ31 alloy by ECAP [8-10,12,15-19]. In the present investigation, the processing was carried out at 453K using a solid die with round channels of 10 mm diameter. The angle between the channels was 110° and the external curvature at the intersection between the channels was ~20°. This geometry imposes a strain in each pass of ~0.8 [20]. A lubricant was used to reduce friction between the billets and the die. Each billet was pressed through a total of 4 passes using route $B_c$ in which the billets are rotated by 90° in the same sense between consecutive passes [21]. A total of four passes was found sufficient to overcome the initial bimodal grain size distribution characteristic of many magnesium alloys processed by ECAP at high temperatures [22].

Rectangular tensile specimens, having cross-sections of 2x3 $mm^2$ and gauge lengths of 4 mm, were machined from the billets both in the as-received condition and after ECAP processing. The gauge lengths of all specimens were parallel to the billet axes.

Tensile tests were conducted using an Instron testing machine adapted with a furnace. Testing was started 15 minutes after the temperature in the furnace stabilized at 623K. A constant rate of crosshead displacement was used in the tests and the testing was performed using initial strain rates of $1.0 \cdot 10^{-4}$, $1.0 \cdot 10^{-3}$, and $1.0 \cdot 10^{-2}$ $s^{-1}$.

All specimens were pulled to failure and then the gauge lengths were mounted in cold resin and carefully ground with abrasive papers and polished with a 0.3 μm and then a 0.05 μm alumina suspension. The polishing was performed with care to a mirror-like finish to avoid any distortions of the cavities within the samples. All samples were observed under optical microscopy and a software for image analysis was used to acquire quantitative data from the cavities. Specifically, the software considered points with gray scale <70 as cavities and >70 as matrix where a gray scale of 0 is black and 255 is white. Similar areas of 1 $mm^2$ were analysed for all specimens at a distance of 1 mm from each fracture tip. In order to cover areas of 1 $mm^2$ along the gauge lengths of each specimen, a total of 20 photographs, each of area 50,000 $\mu m^2$, was recorded at neighbouring areas using a magnification of 100×. The software collected data regarding the area, perimeter and orientation of the longest axis of each cavity. A coefficient of roundness was calculated for every cavity as 4·Area/(Perimeter)$^2$ where the maximum value of 1 corresponds to a perfectly round cavity and less-rounded cavities have lower values. The software excluded any cavities with areas smaller than 1 $\mu m^2$ as this may introduce inaccuracies due to the presence of dirt or small residual scratches.

## 3. EXPERIMENTAL RESULTS

Following the processing by ECAP through 4 passes at 453K, the mean linear intercept grain size

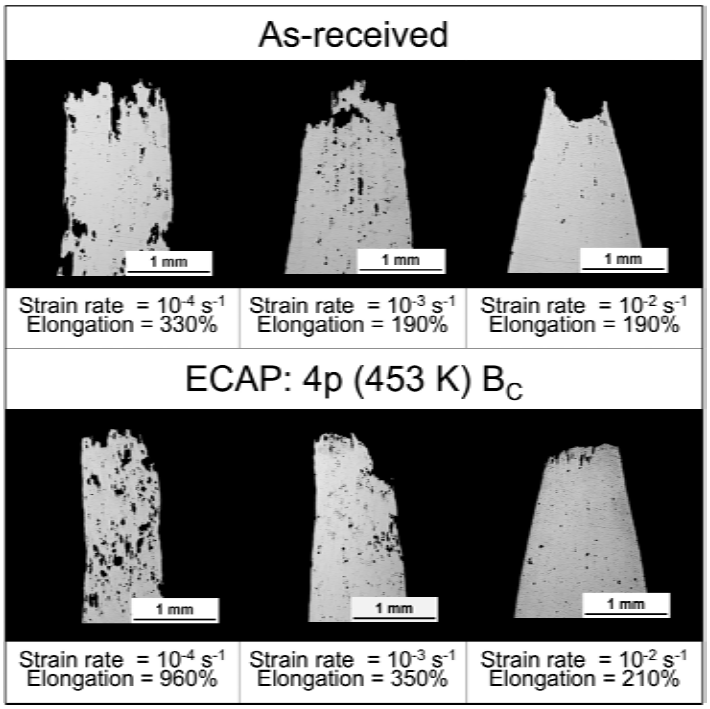


**Fig. 1.** Appearance of the tips of the tensile specimens of the as-received and the ECAP samples after pulling to failure at different strain rates at a temperature of 623K.

was measured as ~2.2 μm which is equivalent to an average spatial grain size of $d \approx 3.8$ μm. Annealing experiments revealed an instability in the microstructures of the as-received and ECAP samples when heating to the tensile testing temperature of 623K. Specifically, the as-received material exhibited a spatial grain size of ~18 μm and the material processed by ECAP exhibited a spatial grain size of ~10 μm after holding for 30 minutes at the testing temperature.

Fig. 1 shows the appearance of the tips of the tensile specimens tested at different strain rates at 623K, where the upper row is for the as-received condition and the lower row is for the samples processed by ECAP. The elongation at failure is also shown for each sample. The dark spots in the material correspond to the cavities and it is therefore apparent that larger cavities are present at the lowest strain rate. By contrast, only a few cavities are visible in the specimens tested at the highest strain rate. The specimen processed by ECAP and tested at $10^{-4}$ $s^{-1}$, which exhibits the highest elongation of 960%, also exhibits the largest and the highest fraction of cavities. The second largest elongation of 350% was observed in the material processed by ECAP and tested at $10^{-3}$ $s^{-1}$ but the total extent of cavitation appears to be lower than in the as-received specimen which exhibited a lower elongation of 190% at the same strain rate.

The area fraction of cavities is shown in Fig. 2 plotted as a function of the initial strain rate for the as-received samples and the material processed by ECAP where the area fraction was obtained by summing the total area of all cavities and dividing by the total area analysed. It is apparent that the area fractions of cavities increase at the lowest strain rate,

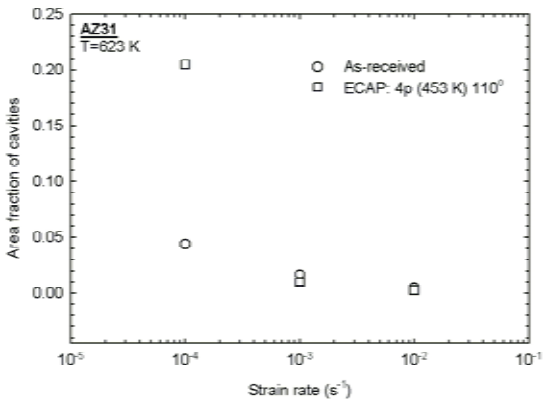


**Fig. 2.** Measured area fraction of cavities in the as-received and the ECAP samples plotted as a function of the strain rate.

especially in the specimen processed by ECAP. However, at the two highest strain rates both the as-received and the ECAP samples exhibit similar area fractions of cavities.

Information on the precise cavity areas is given in Figs. 3 and 4 which show the numbers of cavities plotted as a function of the cavity area for the as received material and the material processed by ECAP, respectively. For this analysis, it was convenient to divide the individual cavity areas into groups corresponding to ranges of 50 $\mu m^2$. Both plots show that the majority of cavities have areas smaller than 50 $\mu m^2$ for both testing conditions. It is also observed that the numbers of cavities tend to increase with decreasing strain rate except only for the lowest strain rate in the as-received material. For example, it can be seen that the numbers of cavities with areas smaller than 200 $mm^2$ is larger in the as-received specimen tested at $10^{-3}$ than at $10^{-4}$ $s^{-1}$ although, as shown in Fig. 2, the latter has a larger area fraction of cavities. This trend occurs because of the relatively large number of cavities having large areas at $10^{-4}$ $s^{-1}$ in the as-received material.

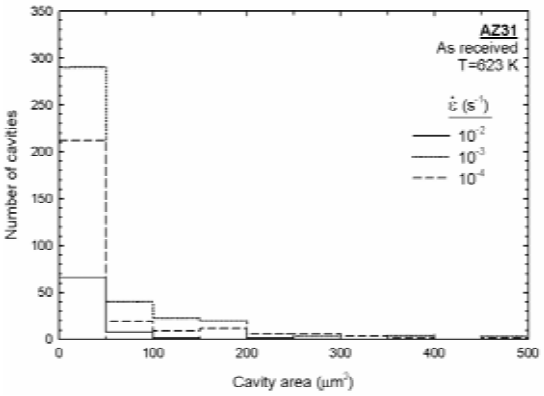


**Fig. 3.** Distribution of cavity areas in the as-received samples after testing at three different strain rates at 623K.

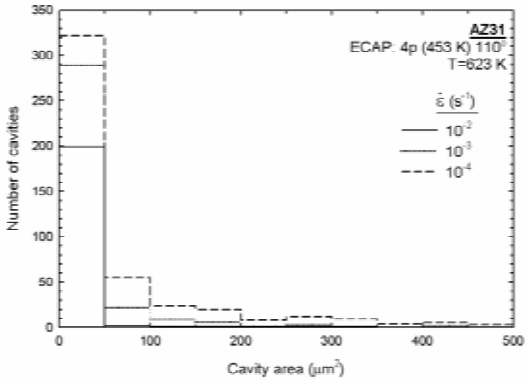


**Fig. 4.** Distribution of cavity areas in the ECAP samples after testing at three different strain rates at 623K.

## 4. DISCUSSION

Numerous investigations have been conducted to measure the cavity morphology and evaluate the rates of cavity growth in materials deforming under high temperature creep and superplastic conditions [23]. The same approach may be used for superplastic materials processed by ECAP.

There are three primary mechanisms of cavity growth in materials tested under high temperature conditions.

First, there is diffusion growth in which cavities grow by the accumulation of vacancies that enter the cavities from the surrounding grain boundary. Under these conditions, the growth rate is given by [24]:

$$\frac{dr}{d\varepsilon} = \frac{2\alpha\Omega\delta D_{gb}}{kT\dot{\varepsilon}r^2}\left(\sigma - \frac{2\gamma}{r}\right), \qquad (1)$$

where $r$ is the radius of the cavity, $\varepsilon$ is the strain, $\alpha$ is a parameter defining the cavity spacing, $\Omega$ is the atomic volume, $\delta$ is the width of the grain boundary, $D_{gb}$ is the coefficient for grain boundary diffusion, $k$ is Boltzmann's constant, $T$ is the absolute temperature, $\dot{\varepsilon}$ is the strain rate, $\sigma$ is the applied stress and $\gamma$ is the free surface energy. Cavities growing by this mechanism tend to be spherical and exhibit no special orientation with respect to the tensile axis.

Second, there is plasticity-controlled growth where growth occurs by plastic flow in the surrounding crystalline matrix. For this mechanism, the rate of growth is given by [25]:

$$\frac{dr}{d\varepsilon} = r - \frac{3\gamma}{2\sigma}. \qquad (2)$$

In practice, cavities growing by plasticity-controlled growth tend to become elongated and to align close to the direction of material flow due to the deformation surrounding the cavities.

In situations where the grain size is exceptionally small, the cavity may intersect several grain boundaries so that the rate of vacancy diffusion into the cavity is enhanced. Under these conditions, the process is termed superplastic diffusion growth and the rate of growth is given by [26]:

$$\frac{dr}{d\varepsilon} = \frac{45\Omega\delta D_{gb}\sigma}{kT\dot{\varepsilon}d^2}, \qquad (3)$$

where *d* is the average grain size. In practice, this becomes a viable mechanism only when the cavity radii are larger than ~*d*/2 where d is the average spatial grain size. The grain sizes in conventional superplastic materials are usually <10 μm but they may reach values of <1 μm in materials processed by ECAP. In these materials, it is reasonable to anticipate that superplastic diffusion will play a major role as a cavity growth mechanism. However, there was a general instability in the microstructures of the AZ31 alloy when testing at 623K, with measured spatial grain sizes in the early stage of deformation of ~18 and ~10 μm for the as-received and the ECAP material, respectively. These larger grain sizes suggest that superplastic diffusion growth will play only a minor role in the cavity growth process for this alloy.

Thus, it follows that diffusion growth and plasticity-controlled growth should represent the dominant cavity growth mechanisms in the present investigation. Inspection of Eqs. (1) and (2) shows that the former mechanism has a rate of growth which is proportional to the reciprocal of the square of the cavity radius while the latter mechanism has a growth rate which is linearly proportional to the instantaneous radius. This means in practice that small cavities will grow by the diffusion mechanism and will appear reasonably rounded whereas the larger cavities will grow by the plasticity-controlled mechanism and become elongated along the tensile axis. In order to validate this conclusion, the easiest procedure is to follow an earlier approach and divide the cavities into ranges of sizes so that the behaviour of the smaller and larger cavities are examined separately [13]. In the following analysis, data are examined separately for the 25% smallest and the 25% largest cavities in each testing condition.

Fig. 5 shows the distributions of the roundness coefficient for the 25% smallest cavities in (a) and (b) and the 25% largest cavities in (c) and (d): Figs. 5a and 5c are for the as-received material and Figs.

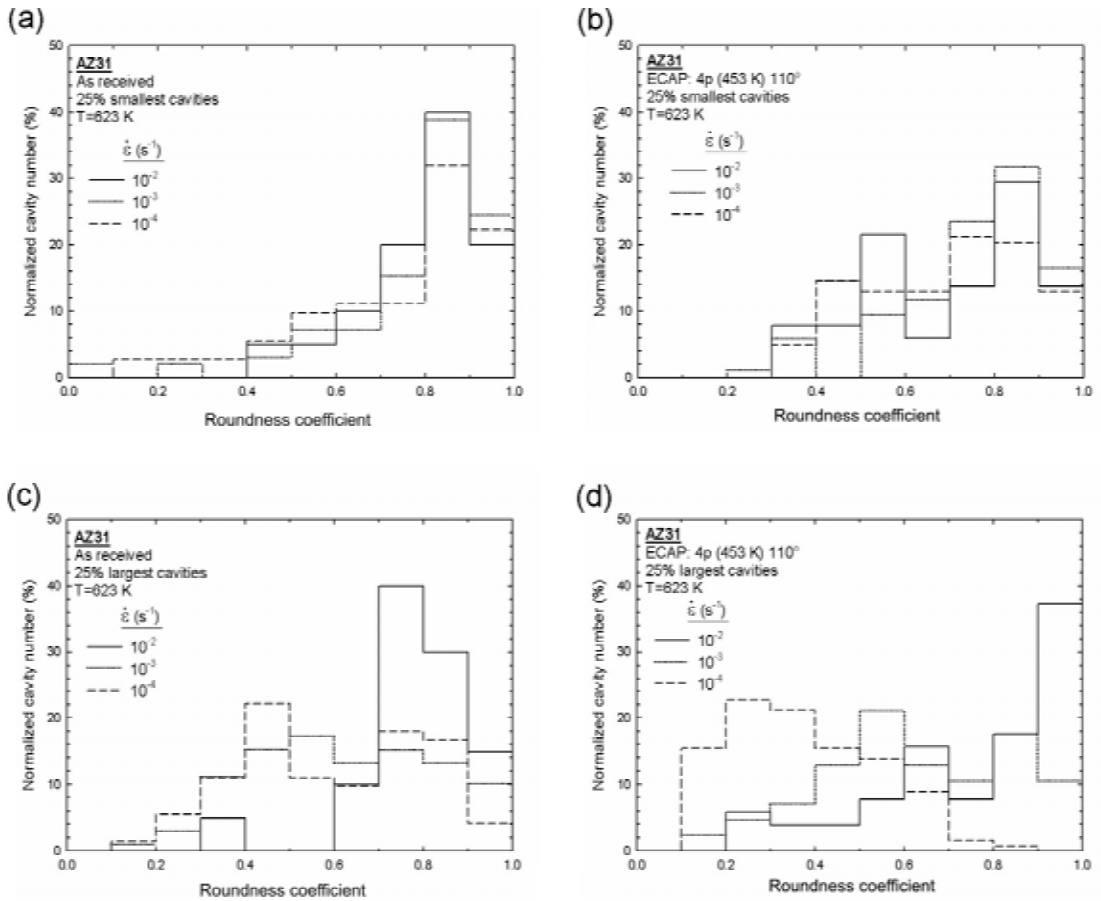


**Fig. 5.** Distributions of cavity numbers as a function of the roundness coefficient for the 25% smallest cavities in (a) and (b) and the 25% largest cavities in (c) and (d): the as-received samples are shown in (a) and (c) and the ECAP samples in (b) and (d).

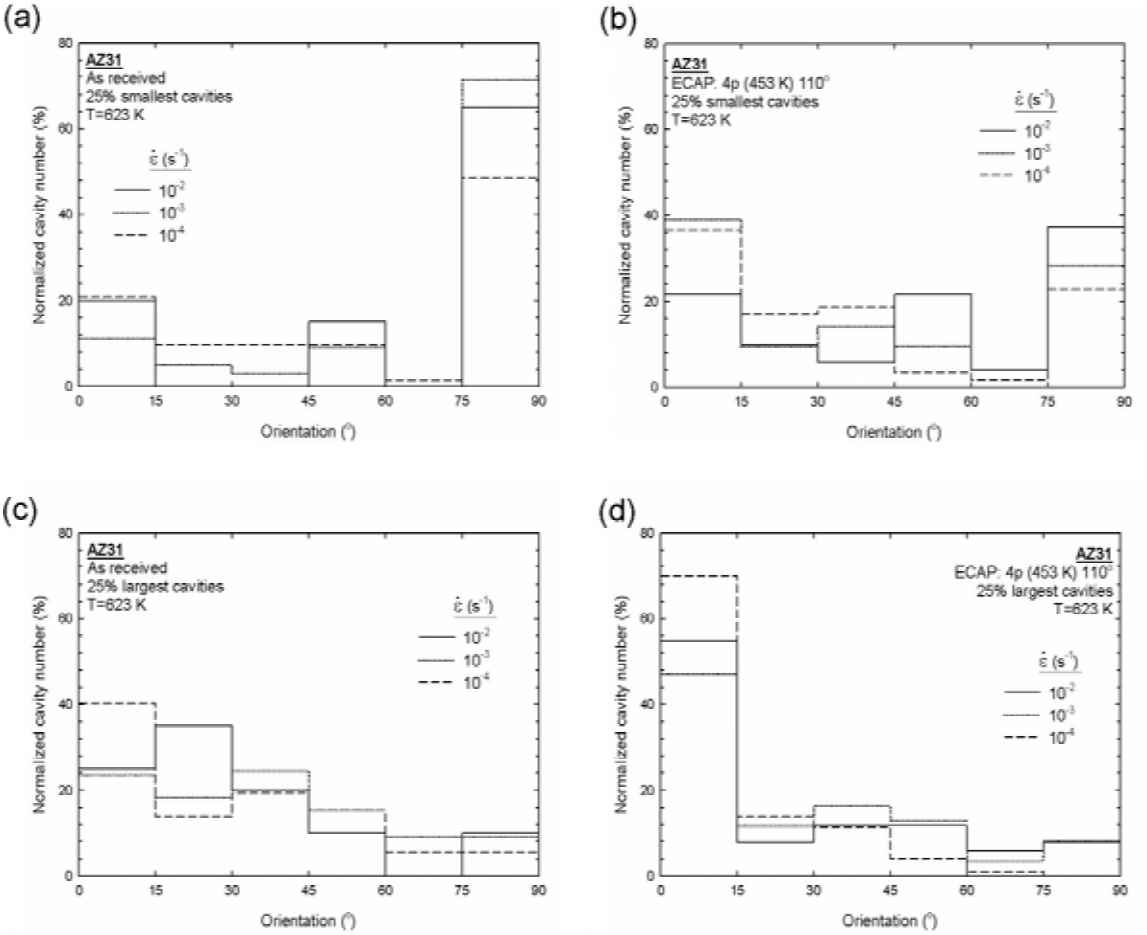


**Fig. 6.** Distributions of cavity numbers as a function of the cavity orientation for the 25% smallest cavities in (a) and (b) and the 25% largest cavities in (c) and (d): the as-received samples are shown in (a) and (c) and the ECAP samples in (b) and (d).

5b and 5d are for the material processed by ECAP. In these plots, a roundness coefficient of 1 corresponds to a perfect circle and lower values denote increasing deviations from a circular morphology. Inspection of Figs. 5a and 5b shows that a major fraction of the smaller cavities exhibit roundness coefficients close to 1 so that these cavities are reasonably rounded. This is consistent with the model for diffusion growth which is expected to play a major role in the growth of the smallest cavities. It is also apparent from Figs. 5c and 5d that the larger cavities exhibit a greater spread in the distribution of roundness coefficients so that they are less-rounded and plasticity-controlled growth plays a more important role. This conclusion is especially supported by the specimen processed by ECAP and tested at the lowest strain rate of $10^{-4}$ $s^{-1}$ which exhibits a peak distribution in Fig. 5d between roundness coefficients of 0.2 and 0.3. Again, this result is consistent with the anticipated behaviour from the models for cavity growth. By contrast, the relatively large fraction of cavities with high roundness coefficients in the ECAP specimen tested at the fastest strain rate indicates that the testing time was too short for the plasticity-controlled growth mechanism to become predominant. The low rate of cavity growth in this specimen is also in agreement with the low area fraction of cavities shown in Fig. 2 and suggests that, as is evident from Fig. 1, cavitation does not play a major role in the failure of this sample. Instead, failure occurs at this fastest strain rate through necking and a general instability.

The dominant mechanism of cavity growth also affects the orientations of the long axes of the cavities with respect to the tensile axis. Fig. 6 shows plots of the normalized cavity number, plotted as a percentage, against the cavity orientation from 0° (lying parallel to the tensile axis) to 90° (lying perpendicular to the tensile axis): Figs. 6a and 6b are for the 25% smallest cavities, Figs. 6c and 6d are

for the 25% largest cavities, Figs. 6a and 6c are for the as-received material, and Figs. 6b and 6d for the ECAP material. It is observed that the smallest cavities in Figs. 6a and 6b exhibit the largest spread in the distribution of angles with some evidence for a relatively larger concentration at the highest angles which may be due to the preferential nucleation of cavities on grain boundaries oriented normal to the tensile axis because of the larger normal stresses. By contrast, the largest cavities in Figs. 6c and 6d show a smaller overall spread and a larger proportion of cavities in the angular range from 0° to 10°. This is in agreement with expectations because in plasticity-controlled growth the cavities grow solely through deformation of the surrounding material.

In summary, therefore, the analysis is fully consistent with the expectations arising from the available cavity growth processes.

## 5. SUMMARY AND CONCLUSIONS

1. A magnesium AZ31 alloy was processed by ECAP and then tested in tension to failure at 623K. Similar tensile testing was also conducted on the as-received alloy.
2. Significant cavitation occurs in this alloy in both the ECAP and the as-received condition at testing strain rates up to $10^{-3}$ $s^{-1}$. Detailed measurements were undertaken to determine the cavity areas and shapes.
3. An analysis shows the cavities grow initially by the diffusion growth process but the morphologies of the larger cavities are consistent with a transition to a plasticity-controlled growth process.

## ACKNOWLEDGEMENT

This work was supported by the National Science Foundation of the United States under Grant No. DMR-0855009.

## REFERENCES

[1] R.Z. Valiev and T.G. Langdon // *Prog. Mater. Sci.* **51** (2006) 881.
[2] M. Kawasaki and T.G. Langdon // *J. Mater. Sci.* **42** (2007) 1782.
[3] A. Yamashita, Z. Horita and T.G. Langdon // *Mater. Sci. Eng.* **A300** (2001) 142.
[4] Z. Horita, K. Matsubara, K. Makii and T.G. Langdon // *Scripta Mater.* **47** (2002) 255.
[5] K. Matsubara, Y. Miyahara, Z. Horita and T.G. Langdon // *Acta Mater.* **51** (2003) 3073.
[6] R.B. Figueiredo, P.R. Cetlin and T.G. Langdon // *Acta Mater.* **55** (2007) 4769.
[7] R.B. Figueiredo and T.G. Langdon // *Adv. Eng. Mater.* **10** (2008) 37.
[8] R.B. Figueiredo and T.G. Langdon // *Mater. Sci. Eng.* **A501** (2009) 105.
[9] R.B. Figueiredo and T.G. Langdon // *J. Mater. Sci.* **43** (2008) 7366.
[10] R. Lapovok, Y. Estrin, M.V. Popov and T.G. Langdon // *Adv. Eng. Mater.* **10** (2008) 429.
[11] C.J. Lee and J.C. Huang // *Acta Mater.* **52** (2004) 3111.
[12] R. Lapovok, T. Williams and Y. Estrin // *Int. J. Mater. Res.* **100** (2009) 609.
[13] M. Kawasaki, C. Xu and T.G. Langdon // *Acta Mater.* **53** (2005) 5353.
[14] M. Kawasaki, Y. Huang, C. Xu, M. Furukawa, Z. Horita and T.G. Langdon // *Mater. Sci. Eng.* **A410-411** (2005) 402.
[15] T. Mukai, M. Yamanoi, H. Watanabe and K. Higashi // *Scripta Mater.* **45** (2001) 89.
[16] H.K. Kim and W.J. Kim // *Mater. Sci. Eng.* **A385** (2004) 300.
[17] H.K. Kim // *J. Mater. Sci.* **39** (2004) 7107.
[18] K. Xia, J.T. Wang, X. Wu, G. Chen and M. Gurvan // *Mater. Sci. Eng.* **A410-411** (2005) 324.
[19] Z. Zúberová, Y. Estrin, T.T. Lamark, M. Janecek, R.J. Hellmig and M. Krieger // *J. Mater. Process. Tech.* **184** (2007) 294.
[20] Y. Iwahashi, J. Wang, Z. Horita, M. Nemoto and T.G. Langdon // *Scripta Mater*. **35** (1996) 143.
[21] M. Furukawa, Y. Iwahashi, Z. Horita, M. Nemoto and T.G. Langdon // *Mater. Sci. Eng.* **A257** (1998) 328.
[22] R.B. Figueiredo and T.G. Langdon // *J. Mater. Sci.* **44** (2009) 4758.
[23] X.G. Jiang, J.C. Earthman and F.A. Mohamed // *J. Mater. Sci.* **29** (1994) 5499.
[24] M.V. Speight and W. Beere // *Metal Sci.* **9** (1975) 190.
[25] J.W. Hancock // *Metal Sci.* **10** (1976) 319.
[26] A.H. Chokshi and T.G. Langdon // *Acta Metall.* **35** (1987) 1089.